Pergamon

Bioorganic & Medicinal Chemistry 10 (2002) 1313–1319

BIOORGANIC & MEDICINAL CHEMISTRY

The 1.76 Å Resolution Crystal Structure of Glycogen Phosphorylase B Complexed with Glucose, and CP320626, a Potential Antidiabetic Drug

Nikos G. Oikonomakos,[a,*] Spyros E. Zographos,[a] Vicky T. Skamnaki[a] and Georgios Archontis[b]

[a]*Institute of Biological Research and Biotechnology, The National Hellenic Research Foundation, 48 Vas. Constantinou Avenue, Athens 11635, Greece*

[b]*Department of Physics, University of Cyprus, Box 20537, CY1678, Nicosia, Cyprus*

Received 29 August 2001; accepted 5 November 2001

Abstract—CP320626, a potential antidiabetic drug, inhibits glycogen phosphorylase in synergism with glucose. To elucidate the structural basis of synergistic inhibition, we determined the structure of muscle glycogen phosphorylase b (MGPb) complexed with both glucose and CP320626 at 1.76 Å resolution, and refined to a crystallographic R value of 0.211 ($R_{free} = 0.235$). CP320626 binds at a novel allosteric site, which is some 33 Å from the catalytic site, where glucose binds. The high resolution structure allows unambiguous definition of the conformation of the 1-acetyl-4-hydroxy-piperidine ring supported by theoretical energy calculations. Both CP320626 and glucose promote the less active T-state, thereby explaining their synergistic inhibition. Structural comparison of MGPb–glucose–CP320626 complex with liver glycogen phosphorylase a (LGPa) complexed with a related compound (CP403700) show that the ligand binding site is conserved in LGPa.

Introduction

CP320626 (Scheme 1), a potential antidiabetic drug, has been shown to be a potent inhibitor of human liver glycogen phosphorylase a (LGPa) and to produce marked glucose lowering in diabetic *ob*/*ob* mice, without altering plasma insulin levels.[1] CP320626 was also demonstrated to be a potent inhibitor of MGPb ($IC_{50} = 334 \pm 10$ nM) and to act in synergism with glucose ($IC_{50} = 178 \pm 10$ nM).[2] The observed synergism could be an important physiological feature of a LGPa inhibitor, because the decrease in inhibitor potency as glucose concentrations decrease in vivo should minimize the risk of hypoglycemia.[3] To understand how CP320626 binds to MGPb, we have recently determined the X-ray structure of MGPb in complex with CP320626 at 2.3 Å resolution.[2] CP320626 binds at a novel allosteric inhibitor site of the enzyme, not previously observed to bind ligands. Furthermore, LGPa was independently reported to bind two related compounds, CP403700 and CP526423, potent inhibitors of the liver isozyme.[4]

Given the potential importance of the detailed interactions of this new class of inhibitors with GP in the structure-assisted design and development of analogous inhibitors, as therapeutic agents for type 2 diabetes therapy,[5] we have cocrystallized MGPb with both CP320626 and glucose and determined the structure of the complex by X-ray crystallographic methods at 1.76 Å resolution. The 1.76 Å resolution structure has

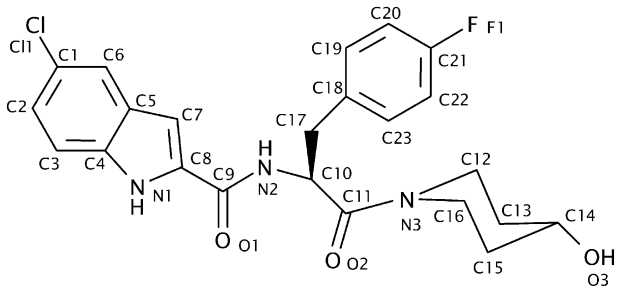

CP-320626

Scheme 1. 5-Chloro-1*H*-indole-2-carboxylic acid [1-(4-fluorobenzyl)-2-(4-hydroxypiperidin-1-yl)-2-oxoethyl]amide (CP320626), showing the numbering system used.

*Corresponding author. Tel.: +30-1-727-3761; fax: +30-1-727-3758; e-mail: ngo@eie.gr

0968-0896/02/$ - see front matter
PII: S0968-0896(01)00394-7

revealed differences in the conformation of the 4-hydroxy-piperidyl moiety of the ligand as compared to the 2.3 Å resolution complex structure. In order to assess the validity of using MGPb as a model for the LGPa in structure-assisted drug design, we have compared the structure of CP320626 complexed with MGPb with the structure of CP403700 bound to LGPa. The structural comparison shows that the MGPb–glucose–CP320626 complex is similar to the LGPa-1–GlcNAc–CP403700 complex in the vicinity of the new allosteric site.

Results and Discussion

The overall architecture of the native T-state MGPb with the location of the catalytic, the allosteric effector, the inhibitor, and the new allosteric inhibitor sites is presented in Fig. 1. Crystallographic data collection processing and refinement statistics for the co-crystallized MGPb–glucose–CP320626 complex are shown in Table 1. The refined $2F_o$–F_c electron density map indicated that CP320626 (Scheme 1) bound at the new allosteric inhibitor site of MGPb located at the subunit interface. Additional density at the catalytic site indicated tight binding of glucose. We describe briefly the MGPb/ligands interactions at the catalytic site and in more detail at the new allosteric inhibitor site.

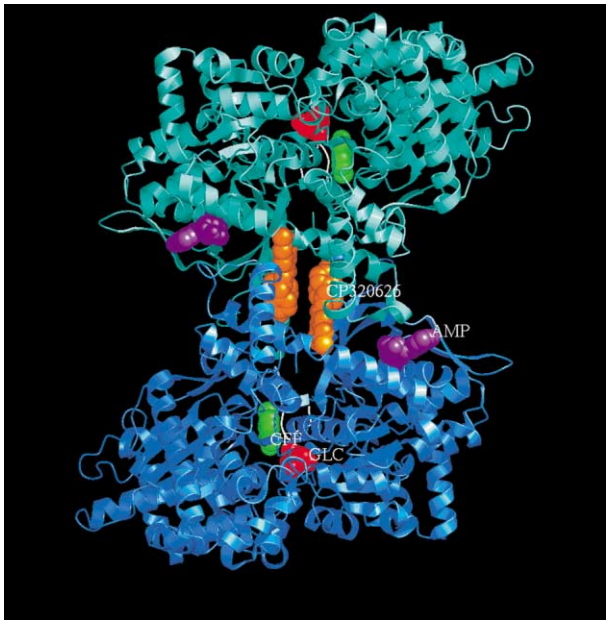

Figure 1. A schematic diagram of the MGPb dimeric molecule viewed down the 2-fold. The positions are shown for the catalytic, allosteric, the inhibitor site, and the new allosteric inhibitor site. The catalytic site, marked by glucose (shown in red), is buried at the centre of the subunit accessible to the bulk solvent through a 15 Å long channel. Glucose, a competitive inhibitor of the enzyme that also promotes the less active T state through stabilisation of the closed position of the 280s loop (shown in white), binds at this site. The allosteric site, which binds the allosteric activator AMP (shown in magenta), is situated at the subunit–subunit interface some 30 Å from the catalytic site. The inhibitor site, which binds purine compounds, such as caffeine (shown in green), is located on the surface of the enzyme some 12 Å from the catalytic site and, in the T state, obstructs the entrance to the catalytic site tunnel. The new allosteric inhibitor site, located inside the central cavity formed on association of the two subunits, binds CP320626 molecule (shown in orange) and is some 15 Å from the allosteric effector site, 33 Å from the catalytic site and 37 Å from the inhibitor site. This figure was produced using XOBJECTS (M.E.M. Noble, unpublished results).

Catalytic site

The mode of binding and the interactions that glucose makes with MGPb in the presence of CP320626 are almost identical with those previously reported for native MGPb.[6] Glucose can be accommodated at the catalytic site of MGPb with essentially no disturbance of the structure and the interactions it makes are similar to those observed in the MGPb–glucose complex.

New allosteric inhibitor site

The electron density maps derived from the previous analysis were interpreted with the 4-hydroxy-piperidyl moiety in $^1C_4$ rather than in $^4C_1$ conformation. The resolution of the present structure allowed us to define more accurately the conformation of the 4-hydroxy-piperidyl moiety (Fig. 2). The 4-hydroxy-piperidyl moiety adopts the most stable puckered ring conformation. In this equivalent chair conformation, the 4-hydroxy-group (O3 in the numbering) of the 4-hydroxy-piperidyl moiety is now axial and not equatorial.

The fitted to the electronic density map $^4C_1$ chair conformation of the CP320626 piperidine moiety was optimized by electronic structure methods described in the

Table 1. Diffraction data and refinement statistics for T-state MGPb–glucose–CP320626 complex

Space group	$P4_32_12$
No. of images (°)	58 (0.8°)[a]
Unit cell dimensions	$a=b=129.0$ Å, $c=116.2$ Å
Resolution range	26.25–1.76 Å
No. of observations	483,106
No. of unique reflections	93,061
$I/\sigma(I)$ (outermost shell)[b]	15.41 (2.33)
Completeness (outermost shell)	95.8% (94.8%)
R_{merge} (outermost shell)[c]	0.054 (0.696)
Outermost shell	1.79–1.76 Å
Refinement (resolution)	26.25–1.76 Å
No. of reflections used (free)	88,308 (4663)
Residues included	13–842
No. of protein atoms	6591
No. of water molecules	355
No. of ligands atoms	15 (PLP)
	31 (CP320626)
	12 (glucose)
Final R (R_{free})[d]	21.1% (23.5%)
R (R_{free}) (outermost shell)	34.2% (36.6%)
r.m.s.d. in bond lengths (Å)	0.007
r.m.s.d. in bond angles (°)	1.25
r.m.s.d. in dihedral angles (°)	24.7
r.m.s.d in improper angles (°)	0.68

[a]0.8° is the rotation range per image.
[b]$\sigma(I)$ is the standard deviation of I.
[c]$R_{merge}=\Sigma_i \Sigma_h \mid <I_h>-I_{ih} \mid / \Sigma_i \Sigma_h I_{ih,}$ where $<I_h>$ and I_{ih} are the mean and ith measurement of intensity for reflection h, respectively.
[d]Crystallographic $R=\Sigma \mid |F_o|-|F_c| \mid / \Sigma |F_o|$, where $|F_o|$ and $|F_c|$ are the observed and calculated structure factor amplitudes, respectively. R_{free} is the corresponding R value for a randomly chosen 5% of the reflections that were not included in the refinement.

Experimental. With both HF and DFT methods the resulting chair structures were very similar and superimposed very well to the X-PLOR-refined geometry. The Cremer–Pople puckering amplitude Q[7] was 0.55–0.54 for all basis sets except HF/3-21G (0.58). This is slightly smaller than the experimental Q value of the cyclohexane chair (0.56), and lies between the theoretical (HF and MP2 ab initio) values for the equatorial (0.59–0.57) and axial (0.56–0.53) forms of piperidine.[8] The configuration around the nitrogen atom of the piperidine moiety (N3) was very similar to the peptide bond geometry obtained for *N*-methyl-acetamide (NMA) by MP2/6-31G* calculations.[9] A small deviation from planarity (less than 10°) was observed in the HF/6-31+G* and 6-311+G* basis structures. Deviations from planarity (up to 10° for the O–C–N–H dihedral) have been also reported in peptide bond ab initio calculations.[10] The optimized structures from both methods superimpose very well to the X-PLOR-refined geometry for the piperidine moiety. Fitting of the entire CP320626 ligand to the density map depends on the configuration of the piperidine moiety, and is optimal for an approximately planar piperidine conformation around the nitrogen atom, as in the optimized structures.

The bound conformation of CP320626 appears to be stabilized by intermolecular contacts to the protein, and there are no intramolecular hydrogen bonds. Straightforward energy minimization using the program SYBYL (SYBYL Molecular Modelling Software, Tripos Associates Inc., T.A. St. Louis, USA 1992) (with the Powell minimiser and default parameters) resulted in a significantly different structure. In the bound CP320626 structure the torsion angles N1–C8–C9–O1 and C7–C8–C9–O1 are 1.6 and 179.8°, respectively, so that the conformation about the C8–C9 bond is significantly different from that in the computed structure (−177.4 and 4.1°) of CP320626. In addition, the conformations about the N2–C10, C10–C17 and C10–C11 bonds are different in the two molecules (the torsion angles C9–N2–C10–C11, C9–N2–C10–C17, N2–C10–C11–O2, and N2–C10–C17–C18 are −61.3 and −116.7°, −179.6 and 124.0°, −59.9 and −102.3°, 179.5 and −85.7°, respectively for the bound and the computed CP320626 molecule).

The values 179.5 and 75.7° for the dihedral angles N2–C10–C17–C18 and C19–C17–C18–C19 in the bound conformation correspond to frequently populated rotamer states of the χ_1 and χ_2 angles for Tyr and Phe residues, as follows by analysis of backbone-independent and backbone-dependent rotamer libraries of protein structures from the PDB.[11]

The binding of CP320626 to MGPb, in the presence of glucose, does not promote extensive conformational changes except for the small shifts of the atoms surrounding the inhibitor, that is of residues 60, 64, and 191 that undergo conformational changes to accommodate the ligand. CP320626 on binding at the new allosteric inhibitor site of MGPb makes a total of seven hydrogen bonds and exploits 114 van der Waals interactions, 41 of which are interactions between nonpolar groups; there are in total 44 contacts to the symmetry related subunit (Table 2). The high resolution structure indicated six well ordered structural waters that form a network of hydrogen bonds that link CP320626 to protein residues; these waters were not observed in the 2.3 Å resolution structure. Thus, Wat267 mediates two polar contacts between the indolecarboxy carbonyl O1 and main-chain O of Asn187 and Glu190 (Fig. 3). Wat257′ makes a direct hydrogen bond to OG1 of Thr38′ (where the prime refers to waters or residues from the symmetry-related subunit). There is a hydrogen bond from the N2 of the carboxamide to the main-chain O of Thr38′. Wat263 contacts NH1 of Arg60, which shifts on binding of CP320626 to GPb. Wat323′ hydrogen-bonds main-chain N of Tyr185′ and main-chain N of Gly186′. These residues make van der Waals contacts with C13 and C14 atoms of the 4-hydroxy-piperidyl moiety. Wat334′ also makes an indirect hydrogen bond to main-chain O of Gly186′ through another new water molecule (Wat300′). These water molecules appear to contribute to CP320626 binding and also stabilize the T state.

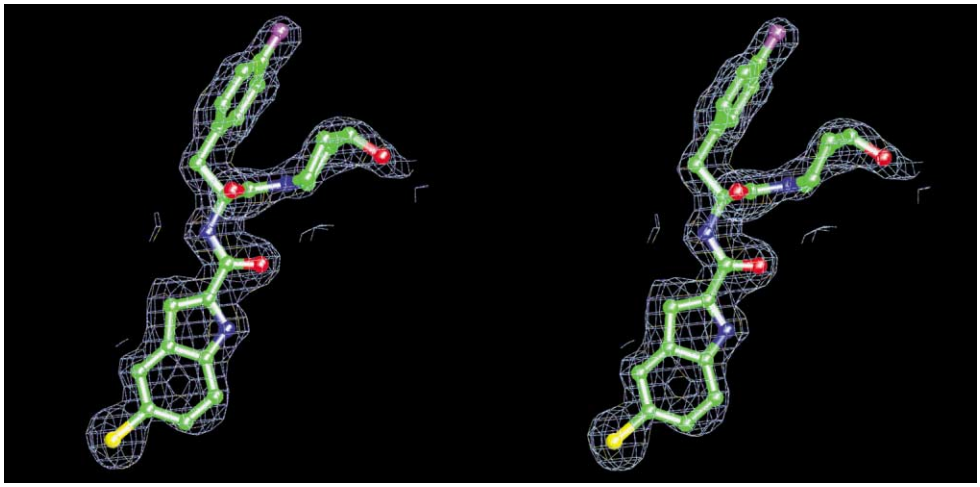

Figure 2. Stereo diagram of the electron density of the bound CP320626 to GPb from a 1.76 Å simulated annealing omit map (contoured at 2.5σ level) with coefficients (F_o-F_c) map. The refined structure of CP320626 is shown. This figure was produced using XOBJECTS (M.E.M. Noble, unpublished results).

Table 2. Hydrogen bonds and van der Waals contacts between the CP320626 and residues of the new allosteric binding site of MGPb[a]

A. Hydrogen bonds Inhibitor atom	Protein atom	Distance (Å)
N1	Glu190 O	2.8
O1	Wat267	2.9
	Wat155	3.0
N2	Thr38′ O	3.0
O2	Lys191 NZ	3.0
N3	Wat155	3.2
O3	Wat89	2.8

B. Van der Waals contacts Inhibitor atom	Protein atom	No. of contacts
CL1	Arg60 O,CG; Leu63 CB; Val64 N,CA,CG2; Trp67 CE3,CZ3	8
C1	Arg60 CG,NE,CD; Trp67 CE3,CZ3; Val40′ CG2	6
C2	Arg60 CG,CD; Trp67 CZ3; Trp189 O; Pro229 CD,CG	6
C3	Arg60 CD; Pro188 O; Trp189 O,C; Glu190 C,O	6
C4	Arg60 NE,CD,CZ,NH2; Pro188 O; Glu190 O; Lys191 CB	7
N1	Arg60 CZ,NH2; Pro188 O; Glu190 C; Lys191 CA,CB; Wat267	7
C5	Arg60 NE,CD,CZ,NH1,NH2; Val40′ CG2	6
C6	Arg60 CG,NE,CD; Val64 CG2; Val40′ CG2; Wat230	6
C7	Arg60 NE,CZ,NH1,NH2; Lys191 CD; Thr38′ O; Val40′ CG2	7
C8	Arg60 CZ,NH1,NH2; Glu190 O; Lys191 CD	5
C9	Lys191 CD; Thr38′ O; Wat267	3
C10	Thr38′ O	1
C11	Wat155	1
O2	Lys191 CD,CE,NZ	3
C12	Ala192 CB; Wat155; Wat229	3
C13	Tyr185′ O; Wat229; Wat348′	3
C14	Gly186′ CA	1
O3	Wat348′	1
C16	Wat155	1
C17	Thr38′ O,CG2; Leu39′ CD1	3
C18	His57′ CE1,NE2	2
C19	His57′ CE1,NE2; Wat211′	3
C20	His57′ CE1,NE2; Wat211′; Wat267′	4
C21	Phe53′ CE2; Pro188′ N	2
F1	Phe53′ CE2; Gly186′ O,C,CA; Asn187′ C,O,N,CA; Pro188′ CA,CB,N,CG,CD	13
C22	Phe53′ CG,CD2,CE2,CZ; Tyr185′ O	5
C23	Leu39′ CD1; His57′ CE1	2
Total		114

[a]Wat89 is hydrogen bonded to Tyr226 OH (3.2 Å) and to Wat154 (3.1 Å); Wat154 is in turn hydrogen bonded to Glu190 OE1 (2.8 Å); Wat155 is hydrogen bonded to Ala192 N (2.6 Å) and to Wat154 (3.0 Å); Wat267 is hydrogen bonded to both Asn187 O (3.0 Å) and Glu190 O (3.3 Å).

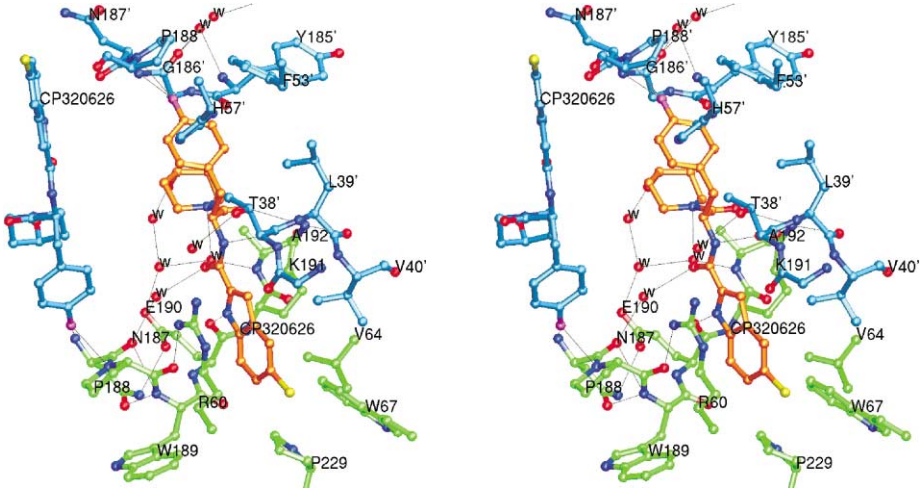

Figure 3. Interactions between CP320626 and MGPb and water structure in the vicinity of the new allosteric site. Residues from subunit 1 are shown in green and their symmetry-related equivalents (from subunit 2) are shown in cyan. Hydrogen bonds are represented as dotted lines and water molecules as red spheres. This figure was produced using XOBJECTS (M.E.M. Noble, unpublished results).

Mechanism of synergistic inhibition

Kinetic experiments on the separate and combined effects of CP320626 and glucose have shown that CP320626 and glucose exhibit synergy in inhibiting MGPb.[2] Our experimental complex structure confirms these observations and shows how both ligands, CP320626 and glucose, stabilize the less active T state. The extensive non-polar contacts and the seven hydrogen bonds from the inhibitor to the protein strengthen the subunit–subunit interface and lock it in a conformation close to the T state quaternary conformation. Thus CP320626 acts as a potent allosteric inhibitor binding at a site distant from the catalytic site and exerting its effects by promoting the T state conformation, consistent with the Monod–Wyman–Changeux[12] model for allosteric proteins. Glucose, bound at the catalytic site, interacts with the side chains of Asp283 and Asn284 holding the 280s loop (residues 282–286) in its closed T-state conformation. By their dual action CP320626 and glucose hold the 280s loop in the inactive conformation and block access to the catalytic site. Therefore by promoting the T state, CP320626 will also promote synergistic glucose binding.

Comparison with LGPa-1-GlcNAc-CP403700 complex in the T-state

Human LGPa is the more important target enzyme in terms of treatment of type 2 diabetes because of its direct influence on blood sugar level. The human LGPa polypeptide chain is 846 residues long, compared with human MGPb of 841 residues and rabbit MGPb of 842 residues. The muscle and liver enzymes are 79% identical with 100% identity at the glucose binding site (at the catalytic site), but the two isoenzymes differ in allosteric properties.[13,14] From a comparison of the amino acid sequences of all phosphorylases, we have found that all but one—Ala192 is serine in the human liver isozyme—of the residues that make up the CP320626 binding site in the rabbit MGP are highly conserved in human LGP and, based on this observation, we suggested that the new allosteric site is likely to be the same in the liver enzyme.[2] The recent crystal structures of human T-state LGPa in complex with CP403700 or CP526423 and 1-GlcNAc, a glucose analogue inhibitor of rabbit MGP[15] verified our hypothesis.

The superposition of the LGPa-1–GlcNAc–CP403700 complex structure with MGPb–glucose–CP320626 complex structure over well defined residues 23–249, 260–313, 326–830 gave r.m.s. deviation of 0.537 Å for C_α atoms, indicating that the two structures have very similar overall conformations. Furthermore, the superimposition of the CP403700 complex with the CP320626 complex over 27 residues of the new allosteric inhibitor site (37′–40′, 53′–57′, 60–67, 188–192, 185′–188′, and 229) gave r.m.s. deviations of 0.307, 0.300, and 0.978 Å for C_α, main chain, and side chain atoms, respectively, indicating that the two structures superimpose well and they closely resemble in the vicinity of the new allosteric site (Fig. 4).

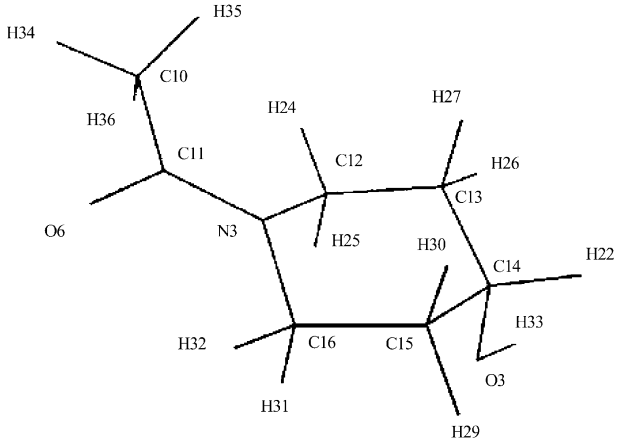

Scheme 2. The molecule 1-acetyl-4-hydroxy-piperidine employed for the geometry optimisation of the piperidine moiety of CP320626, with the numbering system used.

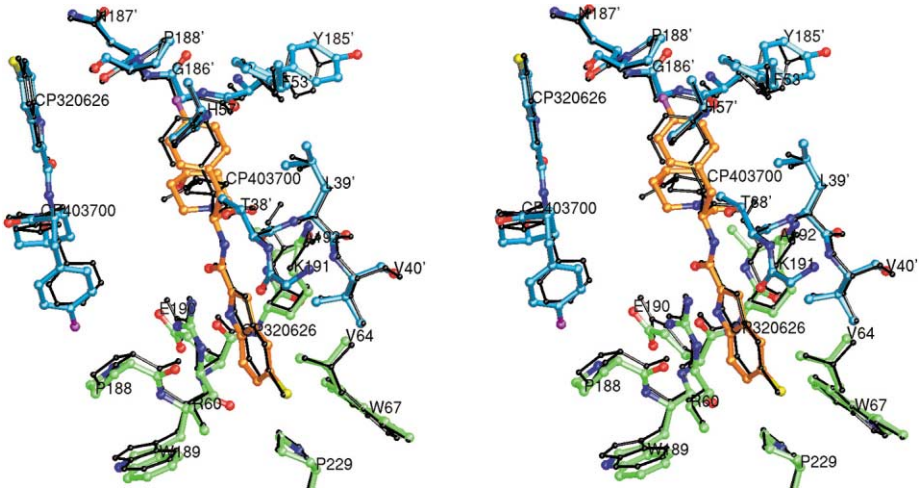

Figure 4. Stereodiagram showing a comparison of CP320626 bound to MGPb–glucose complex with bound CP403700 to LGPa-1–GlcNAc complex (code 1exv) in the vicinity of the new allosteric inhibitor site. Green: MGPb–glucose–CP320626 complex (subunit 1); cyan: MGPb–glucose–CP320626 complex (subunit 2); black: LGPb-1–GlcNAc–CP403700 complex. This figure was produced using XOBJECTS (M.E.M. Noble, unpublished results).

In conclusion, the higher resolution structure, and electronic structure calculations enable for a more accurate determination of the conformation of the 4-hydroxy-piperidyl moiety of CP320626 and water structure. The environment of new allosteric site is similar in the MGPb complex compared to the LGPa complex, indicating the accuracy of MGPb as a model in the design and optimisation of indole-2-carboxamide inhibitors.

Experimental

Crystallization and data collection

Tetragonal ($P4_32_12$) MGPb–glucose–CP320626 crystals were grown as described previously[2] with 50 mM glucose. Crystallographic data were collected from a single crystal, on an image plate on the beamline X31 at Hamburg ($\lambda = 1.05$ Å), at a maximum resolution of 1.76 Å. Crystal orientation and integration of reflections were performed using DENZO.[16] Inter-frame scaling, partial reflection summation, data reduction and post-refinement were all completed using SCALEPACK.[16]

Refinement

Crystallographic refinement of the MGPb–glucose–CP320626 complex was performed with X-PLOR version 3.8[17] using bulk solvent corrections. All data between 26.25 and 1.76 Å were included with no sigma cut-off. The starting protein structure was the 2.3 Å resolution refined model of the MGPb–CP320626 complex. The Fourier maps calculated with SIGMAA[18] weighted (2m***F***o-D***F***c) and (***F***o-***F***c) coefficients indicated tight binding of CP320626 at the new allosteric site and glucose at the catalytic site. Map interpretation was performed using the program O.[19] A few side chains of the enzyme model were adjusted and water molecules were added to the atomic model and retained only if they met stereochemical requirements. The final model was refined by the conventional positional and restrained individual *B*-factor refinement protocol in X-PLOR to give a final *R* factor value of 21.1% ($R_{free} = 23.5\%$). The structure contains residues 13–254, 260–314, 324–837 and 355 water molecules. A Luzatti plot[20] suggests an average positional error of approximately 0.23 Å. The model displays good stereochemistry as determined by PROCHECK[21] with 89.5% of residues in the most favoured regions.

The structure was analysed with the graphics program O.[19] Hydrogen-bonds were assigned if the distance between the electronegative atoms was less than 3.3 Å and if both angles between these atoms and the preceding atoms were greater than 90°. Van der Waals interactions were assigned for non-hydrogen atoms separated by less than 4 Å. R.m.s. deviations in C_α, main chain, and side-chain atoms positions were determined using the program LSQKAB.[21] Coordinates for the 1.76 Å resolution T-state MGPb–glucose–CP320626 complex have been deposited with the RCSB Protein Data Bank (http://www.rcsb.org/) (code 1h5u).

CP320626 geometry optimization

Geometry optimization of a model molecule (1-acetyl-4-hydroxy-piperidine; Scheme 2), approximating the piperidine moiety of the inhibitor CP320626, was performed by ab initio and Density Functional Theory methods with the program Gaussian.[22] Ab initio optimizations were carried out at the Hartree-Fock (HF) level, using the 3-21G, 6-31G*, 6-31+G*, 6-311+G* basis sets. The Density Functional Theory (DFT) calculations used the Becke's three-parametric hybrid exchange functional[23a] with the Lee–Yang–Parr correlation functional (B3LYP),[23b] and the same basis sets as for HF, except 3-21G. Frequency calculations ensured that the optimized structures corresponded to energy minima.

Acknowledgements

This work was supported by the Greek GSRT (PENED1999, 99ED237), the Joint Research and Technology project between Greece and Cyprus (2001–2003) (to N.G.O and G.A.), and EMBL, Hamburg Outstation (HPRI-CT-1999-00017). We wish to acknowledge the assistance of the staff at EMBL, Hamburg, for providing excellent facilities for X-ray data collection.

References and Notes

1. Hoover, D. J.; Lefkowitz-Snow, S.; Burgess-Henry, J. L.; Martin, W. H.; Armento, S. J.; Stock, I. A.; McPherson, R. K.; Genereux, P. E.; Gibbs, E. M.; Treadway, J. L. *J. Med. Chem.* **1998**, *41*, 2934.
2. Oikonomakos, N. G.; Skamnaki, V. T.; Tsitsanou, K. E.; Gavalas, N. G.; Johnson, L. N. *Structure* **2000**, *8*, 575.
3. Martin, W. H.; Hoover, D. J.; Armento, S. J.; Stock, I. A.; McPherson, R. K.; Danley, D. E.; Stevenson, R. W.; Barrett, E. J.; Treadway, J. L. *Proc. Natl. Acad. Sci. U.S.A.* **1998**, *95*, 1776.
4. Rath, V. L.; Ammirati, M.; Danley, D. E.; Ekstrom, J. L.; Gibbs, E. M.; Hynes, T. R.; Mathiowetz, A. M.; McPherson, R. K.; Olson, T. V.; Treadway, J. L.; Hoover, D. J. *Chem. Biol.* **2000**, *7*, 677.
5. Treadway, J. L.; Mendys, P.; Hoover, D. J. *Exp. Opin. Invest. Drugs* **2001**, *10*, 439.
6. Martin, J. L.; Withers, S. G.; Johnson, L. N. *Biochemistry* **1990**, *29*, 10745.
7. Cremer, D.; Pople, J. A. *J. Am. Chem. Soc.* **1975**, *97*, 1354.
8. Carballeira, L.; Perez-Juste, I. *J. Comp. Chem.* **1998**, *19*, 961.
9. Guo, H. G.; Karplus, M. *J. Phys. Chem.* **1992**, *96*, 7273.
10. Sulzbach, H. M.; Schleyer, P. R.; Schaefer, H. F., III. *J. Am. Chem. Soc.* **1995**, *117*, 2632.
11. Dunbrack, R. L., Jr; Karplus, M. *J. Mol. Biol.* **1993**, *230*, 543.
12. Monod, J.; Changeux, J.-P.; Jacob, F. *J. Mol. Biol.* **1965**, *12*, 88.
13. Board, M.; Hadwen, M.; Johnson, L. N. *Eur. J. Biochem.* **1995**, *228*, 753.
14. Rath, V. L.; Ammirati, M.; LeMotte, P. K.; Fennell, K. F.; Mansour, M. N.; Danley, D. E.; Hynes, T. R.; Schulte, G. K.; Wasilko, D. J.; Pandit, J. *Mol. Cell* **2000**, *6*, 139.
15. Oikonomakos, N. G.; Kontou, M.; Zographos, S. E.;

Watson, K. A.; Johnson, L. N.; Bichard, C. J. F.; Fleet, G. W. J.; Acharya, K. R. *Protein Sci*. **1995**, *4*, 2469.
16. Otwinowski, Z.; Minor, W. *Methods Enzymol*. **1997**, *276*, 307.
17. Brunger, A. T. *X-PLOR Version 3.1. A System for X-ray Crystallography and NMR*; Yale University Press: New Haven and London, 1992.
18. Read, R. J. *Acta Crystallogr*. **1986**, *A42*, 140.
19. Jones, T. A.; Zou, J. Y.; Cowan, S. W.; Kjeldgaard, M. *Acta Crystallogr*. **1991**, *A47*, 110.
20. Luzatti, V. *Acta Crystallogr*. **1952**, *5*, 802.
21. Laskowski, R. A.; MacArthur, M. W.; Moss, D. S.; Thornton, J. M. *J. Appl. Crystallogr*. **1993**, *26*, 283.
22. Anon. *Gaussian98*; Gaussian, Inc: Pittsburgh PA, 1998.
23. (a) Becke, A. D. *J. Chem. Phys*. **1993**, *98*, 1372. (b) Lee, C.; Yang, W.; Parr, R. G. *Phys. Rev*. **1988**, *B37*, 785.